

# ASCA Observations of the Seyfert 2 Galaxy NGC 7582: An Obscured and Scattered View of the Hidden Nucleus

Sui-Jian XUE<sup>1,2</sup>, Chiko OTANI<sup>1</sup>, Tatehiro MIHARA<sup>1</sup>, Massimo CAPPI<sup>1,3</sup>, and Masaru MATSUOKA<sup>1</sup>,

<sup>1</sup> *The Institute of Physical and Chemical Research (RIKEN), 2-1 Hirosawa, Wako, Saitama 351-01, Japan*  
E-mail: xue@crab.riken.go.jp

<sup>2</sup> *Beijing Astrophysics Center (BAC), Beijing 100871, China*

<sup>3</sup> *Istituto per le Tecnologie e Studio Radiazioni Extraterrestri (ITeSRE), CNR, iVia Gobetti 101, I-40129 Bologna, Italy*

(Received 1998 January 14; accepted 1998 August 24)

## Abstract

We present the results of two ASCA observations of the Seyfert 2 galaxy NGC 7582. The observation in 1996 revealed the variability at >99% confidence with the shortest timescale of  $\sim 2 \times 10^4$  s. Variations were significant only in the hard X-ray band (2–10 keV) with the normalized variability amplitude  $\sigma_{RMS} \approx 0.3$ , which is the same level as that of Seyfert 1 galaxies of the same luminosity. In the soft X-ray band (0.5–2 keV) the flux stayed almost constant. The source showed similar variability in another shorter observation in 1994.

The overall broadband (0.5–10 keV) spectrum is complex. It shows a heavily absorbed ( $N_H \sim 1.0 \times 10^{23} \text{ cm}^{-2}$ ) and flat ( $\Gamma \sim 1.5$ ) power-law continuum plus a slightly broad iron  $K\alpha$  line at  $\sim 6.4$  keV with  $EW \sim 170$  eV. Below 2 keV, a “soft excess” emission dominates the spectrum.

No significant variations in the average continuum and line fluxes were detected between the two observations. However, the inferred column density increased by  $\sim 4 \times 10^{22} \text{ cm}^{-2}$  from 1994 to 1996. This variation could be interpreted in terms of “patchy torus”, namely suggesting that absorbing material on our line-of-sight comprises many individual clouds. The observed iron line feature is also consistent with the picture of the transmission of nuclear X-ray continuum through the torus-like geometry. The nuclear X-ray luminosity (2–10 keV) is  $\sim 3 \times 10^{42} \text{ ergs s}^{-1}$ , similar to the typical values for Seyfert 1 galaxies.

The constant 0.5–2 keV soft X-ray spectrum, though at least partially accounted for by some starburst contribution, could be interpreted mostly as the scattered central continuum from a spatially extended region. This is consistent with the lack of rapid soft X-ray variability. Thus NGC 7582 is a typical example of a type 2 Seyfert galaxy which exhibits both an obscured and scattered emission component as expected from the AGN unification model.

**Key words:** Galaxies: individual (NGC 7582) – Galaxies: Seyfert 2 – Galaxies: X-ray

## 1. Introduction

NGC 7582 is a nearby ( $z = 0.0053$ ) active galaxy in the southern sky, one of the four spiral galaxies forming the Grus Quartet. Though it is categorized as a Seyfert 2 galaxy according to its optical spectrum, it also joins a small class of so called “narrow emission line galaxies” (NELG) which appear to have relatively bright and variable X-ray luminosity. In a recent optical spectropolarimetry survey carried out by Heisler et al. (1997), no scattered broad-emission lines were detected in NGC 7582. They interpreted this as seeing through an edge-on obscuring torus, providing that scattering particles polarizing broad-line photons lie very close to or possibly within the plane of the torus.

In X-ray band, there are a number of studies on NGC

7582 based on previous space missions, e.g. HEAO-1/A2 (Mushotszky 1982), Einstein (Maccacaro & Perola 1981; Reichert et al. 1985), EXOSAT (Turner & Pounds, 1989), and more recent Ginga (Warwick et al. 1993). These studies have suggested that NGC 7582 most probably contains an obscured or highly absorbed (with column density  $N_H > 10^{23} \text{ cm}^{-2}$ ) X-ray emission nucleus, like a typical type 2 Seyfert galaxy. However, some striking results were also revealed, especially that large factors of variabilities in the absorption column density as well as in the continuum flux occurred during one or between some observations. These results could be the important key to investigate the nature of the absorbing matter along the line-of-sight, as well as to test the AGN unification scheme in this special object. Unfortunately, these results are difficult to be interpreted, because several bright

X-ray sources were detected by Einstein and ROSAT HRI in the immediate proximity of NGC 7582, including cluster Sérsic 159-03 (Abell S1101), active galaxies NGC 7590, NGC 7552 (Charles & Philips, 1982), and a BL Lac object PKS 2316-423 (Crawford & Fabian 1994), which probably contaminated the former non-imaging X-ray observations. Therefore, to clarify the possible variability properties of NGC 7582, multiple, spectral imaging X-ray observations (with spatial resolution sufficient to separate out the confusing sources in the field) are ideally required.

In this paper, we present the results of two ASCA observations of NGC 7582. The imaging capability of ASCA clearly separated these 5 sources. The broad energy band (0.5–10 keV) X-ray spectra obtained with ASCA provide a good opportunity to improve our understanding of this object significantly. We describe the observations and data reduction in section 2. The high quality data enables temporal and spectral analysis, which are presented in section 3 and section 4, respectively. The results are discussed in section 5. The conclusions of the paper are given in section 6.

## 2. Observations and data reduction

NGC 7582 was observed twice with the ASCA satellite. One observation was carried out on November 21-22, 1996 (AO4, hereafter), with Solid-state Imaging Spectrometers, SIS-0 (S0) and SIS-1 (S1) operating in 1-CCD Faint mode. The other one was made on November 14, 1994 (AO2 hereafter), with the SIS instruments operating in a mixture of Bright and Faint 2-CCD modes. For each observation, Gas Imaging Spectrometers, GIS-2 (G2) and GIS-3 (G3) were operated in normal PH mode. All data were selected from the intervals of high and medium telemetry rates. The SIS data were screened using the following criteria: a) The data was taken outside of the South Atlantic Anomaly, b) the angle between the field of view and the edge of the bright and dark earth exceeded  $25^\circ$  and  $5^\circ$ , respectively, and c) the cutoff rigidity was greater than  $4 \text{ GeV } c^{-1}$ . After these selections, we also deleted data if d) there were any spurious events or the dark frame error was abnormal. For GIS data, no bright earth angle and cutoff rigidity criteria were applied. More details concerning the performance and instrumentation of ASCA were reported in separate papers (ASCA satellite: Tanaka et al. 1994; SIS: Burke et al. 1991; GIS: Ohashi et al. 1996).

The resulting effective exposures of the observation in 1996 are  $\sim 41.4$ ks and  $\sim 42.4$ ks for the SIS and GIS, respectively. For the SIS data in mixture mode obtained in 1994, the data was treated in BRIGHT (including converted FAINT data) mode, and the resulting effective exposures of the data are  $\sim 22.5$ ks for the SIS and  $\sim 24.9$ ks for the GIS.

ASCA data of NGC 7582 did not suffer contaminations from any confusing sources noted in section 1. Source counts of both observations were extracted from circular regions of radius  $\sim 3$  arcmin and  $\sim 5$  arcmin for the SIS and GIS, respectively. All the backgrounds were extracted from the source-free regions in the same detectors.

## 3. Timing analysis

Light curves of each observation were extracted for all the four spectral instruments in XSELECT (V1.3), with short (128 s) and long (5760 s,  $\sim 1$  satellite orbit) binnings. Then the same instrumental-type data, SIS0 and SIS1, GIS2 and GIS3 were combined to improve the signal-to-noise ratio. The resulting light curves show that the SIS and GIS data are well consistent in each observation.

The variability properties were further investigated for SIS light curves in the soft (0.5–2 keV) and hard (2–10 keV) energy bands (figure 1). The result indicates that significant variation ( $\sim$  a factor of 2) was only detected in the hard X-ray band with typical timescale of  $\sim 2 \times 10^4$  s, which could be clearly seen on both 128 s and 5760 s temporal analysis (figure 1). On the other hand, the soft X-ray curve almost remained constant during each observation. There was no sign of correlation between the hard and soft light curves. According to the spectral study in the next section, a break-point of the soft and hard components is  $\sim 2$  keV. Together with the temporal analysis, we can conclude the existence of the two independent spectral components in the spectrum of NGC 7582.

In order to check whether there was a possible correlated spectral variability, such as a change of  $N_{\text{H}}$ , within the hard band during each observation, we have calculated the hardness ratio HR (defined as the ratio of the count rate in 4–10 keV to the count rate in 2–4 keV) for each bin of the light curve. The resulting HR is plotted in figure 2 as a function of count rate for the SIS light curve of AO4. It shows no significant spectral variability with the intensity. The same result was obtained for AO2 data.

## 4. Spectral analysis

Since no significant spectral changes were detected in the individual soft and hard spectral components in either observation, we added together the data from each observation and performed spectral fitting of the four time-averaged spectra simultaneously. These spectra are: pairs of the SIS(0/1) in the energy of 0.5–10 keV, and the GIS(2/3) in 0.7–10 keV. The data was analyzed for each year; and independent normalizations were used for

Fig. 1. The comparison of SIS hard and soft band light curves of NGC 7582. Light curves in both short (128 s) and long (5760 s) bins are shown for AO4 (upper panel) and AO2 (lower panel), respectively. The time axis of AO4 starts from 18:24:13, November 21 (UT), 1996; and AO2 starts from 05:47:32, November 14 (UT), 1994. For both observations, the rapid variability is seen in the hard (2–10 keV) band, and no significant correlated variability in the soft (0.5–2 keV) band.

Fig. 2. The hardness ratio (4–10 keV)/(2–4 keV) as the function of SIS count rate (2–10 keV) in AO4. No spectral variability, such as a change of  $N_{\text{H}}$ , was detected in the hard component.

the SIS and GIS data, because there are small uncertainties in the relative flux calibrations of different detectors. The spectra were grouped so that each energy channel contains at least 20 counts allowing minimization  $\chi^2$  techniques. Spectral analysis have been performed using XSPEC(V9.1) program (Arnaud et al. 1991).

Throughout this paper, the Galactic line-of-sight column density is fixed at  $N_{\text{Hgal}} = 1.47 \times 10^{20} \text{ cm}^{-2}$  (Stark et al. 1992). All errors reported below are quoted at the 90% confidence level for one interesting parameter (i.e.  $\Delta\chi^2 = 2.7$ ).

#### 4.1. Modeling of the soft excess component

The broad-band spectra were initially modeled with a single absorbed power-law model. Residuals of the fitting clearly indicate the presence of significant “excess” emission that dominates the spectrum below  $\sim 2$  keV. At higher energies, some small residuals around  $\sim 6.4$  keV indicate the presence of an iron  $K\alpha$  emission and/or an absorption edge.

The poor description of the single power-law and the complexity of overall spectrum might be expected in the physical picture of unified AGN schemes. In the scheme, we might expect to see some fraction of the primary continuum (power-law like) through the heavy obscuration of the putative torus, with some components superimposed upon this, which could represent the indirect central continuum scattered into our line-of-sight, and/or the leakage of the central continuum through a non-uniform (e.g. partial covering) absorber. In addition, hot gas due to the starburst activity or in the host galaxy might also make an extra contribution to the soft X-ray emission. Thus, both the data and the possible physical picture lead us to explore some complex models for NGC 7582.

We then attempt to fit the spectra by adding an extra spectral component to the single power-law to represent the upturn soft X-ray excess below  $\sim 2$  keV. The following continuum models were firstly investigated:

a) Scattering model. This model consists of the sum of two power-laws having the same photon index but different absorptions and normalizations. One power-law is a direct component absorbed by a highly intrinsic column density, and the other is a scattered component which is free from intrinsic absorption. The “non-absorbed” scattered continuum mimics the soft excess. This interpretation is supported by unified models of AGNs (Antonucci, 1993), which predicts that the direct continuum of Seyfert galaxies is strongly obscured by a thick torus (Ghisellini, Haardt, & Matt 1994), whereas a part of the nuclear emission is scattered by free electrons surrounding the broad-line region (e.g. Antonucci & Miller 1985; Awaki et al. 1991). The fraction of the scattered continuum is evaluated by the ratio of the two power-law normalizations  $A_s/A_p$ . The spectral fit of this model is shown in figure 3, and the best-fit parameters are listed in table 1.

It should be noted that the “partial covering model” is numerically equal to the scattering model. In this model, the “non-absorbed” power law component, which might possibly explain the soft excess, physically represents a fraction “leakage” of the continuum from a partially obscured central X-ray source. In contrast to the scattered scenario, the soft component in the partial covering model is expected to show the same rapid variations as the direct continuum. From a correlation analysis of the soft (0.5–2 keV) with hard (2–10 keV) count-rate, the  $1\sigma$  upper limit of contribution from partial covering (i.e. the leakage of variable hard X-ray continuum) to the soft

emission was not more than 10%. Therefore, the partial covering model is immediately excluded by the data. The constancy of the soft component is consistent with the scattering model because any rapid variations in the direct continuum would be smeared out in the emergent spectrum.

In the scattering model, the soft-emission is physically related to the hard-emission component; however there are also a few possibilities that the soft emission is of thermal origin, and is completely independent on the hard-emission component. For example, b) Bremsstrahlung and c) Raymond-Smith model could account for the soft component. In these cases, it is assumed the soft X-ray emission is produced by an optically thin hot plasma associated with the host galaxy, e.g. starburst activities. The best-fit of these two thermal models have minor difference, thus only the result of model c was quoted in table 1.

For each model we have also tested the significance for the presence of a narrow iron  $K\alpha$  line, which was firstly fitted with free energy, and fixed width ( $\sigma$ ). In all these models, thawing the line width could improve the line fitting at  $> 90\%$  confidence level ( $\Delta\chi^2 = 2.7$  for one interesting parameter) than that of narrow line fitting, we then let this parameter free.

It is clear from table 1 that both the scattering and thermal models give acceptable fits to the data with  $\chi^2_\nu = 1.0 \sim 1.1$ , and these models yield similar values of column density, hard photon index and the similar iron  $K\alpha$  feature in each observation dataset. Therefore, statistically these two type of models cannot be discriminated. However, as we will discuss in section 5.3.1, the soft continuum in NGC 7582 cannot be dominated by the thermal component. This suggests that the soft continuum of the source is most likely dominated by the scattered component.

#### 4.2. The Best-fit Model

The complexity of soft component is also suggested by the data. Although the scattering model gives an acceptable fit of the data, it is not perfect. There are still some significant residuals below 1 keV (see figure 3), especially a small bump around 0.85 keV that might be of thermal origin, i.e. probably iron L-shell complex lines. Therefore, we modeled this extra component using the Raymond-Smith model, the best fit gives a the temperature of  $kT \simeq 0.8$  keV, and abundance of 1.0 – 2.0 solar (table 1). Although the abundance is poorly constrained owing to the lack of unambiguous line features in soft X-ray spectrum, the extra two free parameters improved the fit of the scattering model at  $> 99.9\%$  significance level with  $\Delta\chi^2 = 21$ . The best-fit results are listed in table 1 and shown in figure 4. In this complex model, the Raymond-Smith emission contributes at most  $\sim 10 - 20$

% of the flux at 1 keV, which is consistent with the value expected from the FIR/X-ray luminosity correlation for normal and starburst galaxies (see section 5.3.1).

Therefore, the plausible model which explains the data is that the soft emission consists of a mixture of the scattering component and the thermal component; the hard component is a heavily absorbed power-law continuum plus a slightly broad cold iron  $K\alpha$  line. For this model, confidence contours of the photon index of the primary continuum vs. column density are shown in figure 5.

Finally, we have searched for the presence of an iron edge in excess of that modeled by the best-fit absorption in each dataset. Adding two extra parameters (threshold energy and the depth of the edge) to the best-fit model produced a slight improvement to the fit ( $\Delta\chi^2 \simeq 4.6$ ) for AO4, and gave result of  $\tau \simeq 0.15^{+0.15}_{-0.10}$  at  $\sim 7.1$  keV. However, the AO2 data does not suggest any additional iron edge probably due to its lower statistics. In this model, the excess absorption edge implies either an iron overabundance of factor  $\sim 2$  or an additional X-ray absorption (partially covering) column in the line-of-sight (see section 5.3.2).

## 5. Discussions

### 5.1. Short-term variabilities during the observations

Rapid X-ray variability is a very common property of Seyfert 1 galaxies, and the variability amplitude was found anti-correlated with the source luminosity (e.g. Nandra et al. 1997; Lawrence & Papadarkis 1993). Therefore, to examine whether or not Seyfert 2 galaxies (for which we can detect their direct nuclear emission) also show the rapid variability, is a crucial test for the AGN unification scheme.

Furthermore, it is widely examined that the complex X-ray spectra of type 2 Seyferts in the ASCA energy band have different physical origins. To discriminate them, variability studies of various spectra components are important. NGC 7582 is a rare example of Seyfert 2 galaxies that clearly shows rapid X-ray variability. Most compellingly, the hard and soft X-ray emissions of this source have different variability properties that indicate two distinct emission regions: hidden nuclear hard X-ray emission and extended soft X-ray emission.

To test the idea that the observed highly variable continuum comes from a hidden Seyfert 1 nucleus, we added our data points to the  $\sigma^2_{RMS}$  (0.5-10 keV) vs.  $L_X$  (intrinsic luminosity in 2–10 keV) plot of Seyfert 1 samples (Nandra et al. 1997) (figure 6). The rapid-variability characteristics of the hard X-ray component in NGC 7582 at two different epochs are very similar to those of Seyfert 1 galaxies. This suggests that the nuclear emission of NGC 7582 is similar to that of Seyfert 1 galaxies. Turner et al. (1997a) also reported three other Type-2 objects,

Fig. 3. The folded spectrum of NGC 7582, fitted simultaneously for SIS(0/1) and GIS(2/3), with the scattering model. Related residuals for AO4 (upper panel) and AO2 (lower panel) are also shown. The cross marker represents the SIS data, and the void-square denotes the GIS data. The model gives acceptable description of the data (see table 1), but still some residuals remain around  $\sim 1$  keV, indicating that the soft spectrum is more complex than just scattered component.

Table 1. Spectral fit parameters

Data	$kT$ [keV]	Abundance [solar]	$N_{\text{H}}$ [ $10^{23}$ cm $^{-2}$ ]	$\Gamma$	$A_s/A_p^a$ %	$A_{RS}/A_s^b$ %	$E_{K\alpha}$ [keV]	$\sigma$ [keV]	EW [eV]	$\chi^2/\text{d.o.f}$
<b>Scattering + Absorbed Power Law :</b>										
1994	-	-	$0.94^{+0.08}_{-0.08}$	$1.49^{+0.14}_{-0.14}$	$3.9^{+1.7}_{-1.2}$	-	$6.31^{+0.09}_{-0.10}$	$0.12^{+0.35}_{-0.07}$	$170^{+80}_{-65}$	1.07/288
1996	-	-	$1.32^{+0.06}_{-0.06}$	$1.64^{+0.09}_{-0.09}$	$3.2^{+0.9}_{-0.7}$	-	$6.34^{+0.06}_{-0.06}$	$0.15^{+0.11}_{-0.06}$	$192^{+47}_{-46}$	1.05/578
<b>Thermal (RS) + Absorbed Power Law :</b>										
1994	$1.62^{+1.54}_{-0.51}$	< 0.09	$0.75^{+0.05}_{-0.04}$	$1.33^{+0.16}_{-0.16}$	-	-	$6.30^{+0.09}_{-0.1}$	$0.12^{+0.12}_{-0.08}$	$170^{+70}_{-77}$	1.04/288
1996	$2.48^{+1.40}_{-0.60}$	< 0.08	$1.20^{+0.11}_{-0.08}$	$1.52^{+0.13}_{-0.13}$	-	-	$6.33^{+0.07}_{-0.06}$	$0.15^{+0.11}_{-0.06}$	$180^{+53}_{-47}$	1.04/578
<b>Scattering + RS + Absorbed Power Law :</b>										
1994	$0.78^{+0.07}_{-0.12}$	$2.6^{+1.6}_{-1.6}$	$0.86^{+0.08}_{-0.08}$	$1.38^{+0.12}_{-0.11}$	$3.8^{+0.5}_{-1.5}$	$16^{+7}_{-7}$	$6.32^{+0.09}_{-0.10}$	$0.12^{+0.16}_{-0.10}$	$163^{+75}_{-66}$	0.99/286
1996	$0.79^{+0.07}_{-0.09}$	$1.4^{+0.5}_{-0.4}$	$1.24^{+0.06}_{-0.08}$	$1.52^{+0.09}_{-0.07}$	$3.3^{+0.3}_{-0.4}$	$14^{+5}_{-6}$	$6.33^{+0.06}_{-0.05}$	$0.15^{+0.10}_{-0.07}$	$182^{+50}_{-40}$	1.02/574

<sup>a</sup>  $A_s/A_p$  = (normalization of the scattered component at 1 keV)/(normalization of the primary continuum at 1 keV)

<sup>b</sup>  $A_{RS}/A_s$  = (normalization of the RS component at 1 keV)/(normalization of the scattered component at 1 keV)

NGC 526A, MCG-5-23-16 and NGC 7314 that showed the same property as seen in figure 6. This result suggests that rapid X-ray variability is also common in Seyfert 2 galaxies.

### 5.2. Long-term variabilities between the observations

Almost the same average 2–10 keV flux ( $\sim 1.5 \times 10^{-11}$  erg cm $^{-2}$  s $^{-1}$ ) was obtained in two ASCA observations. This flux is consistent with the HEAO 1 result of  $1.4 \times 10^{-11}$  erg cm $^{-2}$  s $^{-1}$  (Mushotzky, 1982), if assumed that the power-law component in their spectral model represents the source emission; and also consistent with the EXOSAT result of  $1.7 \times 10^{-11}$  erg cm $^{-2}$  s $^{-1}$  (Turner & Pounds 1989). Among the previous studies, Ginga observation reported the lowest continuum level as

$\sim 0.6 \times 10^{-11}$  erg cm $^{-2}$  s $^{-1}$  (Warwick et al. 1993); and that a substantial increase in  $N_{\text{H}}$  from  $1.6 \times 10^{23}$  cm $^{-2}$  to  $4.6 \times 10^{23}$  cm $^{-2}$  occurred in the  $\sim 4$  year interval between the EXOSAT and Ginga observations. All these results indicated that a complex long term spectral fluctuation might exist accompanying with a larger factor change in absorption column density.

The two ASCA observations separated 2 years provided a valuable chance to check for spectral variability over a longer time scales. Comparing the contour plots of photon index vs. column density between the two observations in figure 5, the spectral index does not show a significant difference. However, the absorption column density evidently increased by  $\sim 44\%$  from AO2 to AO4, confirming previous findings (Warwick et al. 1993). The present ASCA observations are amongst the best avail-

Table 2. Flux and luminosity for the best-fit model

Dataset	Observed Flux [ $10^{-13}$ erg $\text{cm}^{-2}\text{s}^{-1}$ ]			Intrinsic Luminosity <sup>b</sup> [ $10^{40}$ ergs $\text{s}^{-1}$ ]	
	0.5-2 keV	2-10 keV	2-10 keV <sup>a</sup>	0.5-2 keV <sup>c</sup>	2-10 keV <sup>a</sup>
1994	$3.63^{+0.49}_{-0.67}$	$151^{+36}_{-42}$	$227^{+73}_{-54}$	$4.54^{+0.64}_{-0.71}$	$273^{+89}_{-65}$
1996	$4.18^{+0.34}_{-0.40}$	$155^{+24}_{-22}$	$272^{+46}_{-40}$	$5.06^{+0.66}_{-0.26}$	$327^{+57}_{-46}$

<sup>a</sup>The absorption corrected. <sup>b</sup>Assuming  $H_0 = 50 \text{ km s}^{-1}\text{Mpc}^{-1}$  and  $q_0 = 0.5$ . <sup>c</sup>The Galactic absorption corrected.

Fig. 4. The unfolded spectrum shown for AO4, fitted with the model of “absorbed power-law + scattered power-law + Raymond-Smith + Fe K line”. The best-fit parameters of this model and flux measurements are listed in table 1 and table 2.

able in providing evidence for the variability of X-ray absorbing column within a Seyfert 2 nucleus, because most previous results (see Warwick et al. 1993) are based on a comparison of two measurements made by different instruments.

Variations in X-ray absorbing column are not common events in AGNs. To our knowledge, so far it was only reported for a Seyfert 1.9 galaxy ESO103-G55 by Warwick et al. (1988) based on multi-observations made with EXOSAT. In that case, the significant variation in the column occurred over a 90-day period, the author interpreted it in terms of an X-ray absorbing screen composed of broad-line clouds moving out of the line-of-sight.

However, the significant amount of X-ray absorbing column in type 2 AGN is generally associated with the putative obscuring torus. The partial obscuring of the nucleus of NGC 7582 would occur in the outer region close to the edge of the torus (see section 5.4). If this region contains clumpy clouds (i.e. “patchy torus”), its orbital motion around the nucleus could cause the observed variability of the line-of-sight absorption.

If this is the case, the transverse time scale,  $D/v$ , of a cloud with the size,  $D$ , and the velocity,  $v$ , should be smaller than  $\Delta t \sim 2$  years.  $\Delta t$  should also be larger than 1 week, since no variation of the column density was observed within one previous observation. As the velocity is estimated by  $(GM/R)^{1/2}$ , where  $R$  is the distance from the nucleus and  $G$  is the gravitational constant, this gives

$$D_{pc} \lesssim \Delta t (GM/R)^{1/2} \sim 1.3 \times 10^{-3} M_8^{1/2} R_{pc}^{-1/2}, \quad (1)$$

$$D_{pc} \gtrsim 1.3 \times 10^{-5} M_8^{1/2} R_{pc}^{-1/2}, \quad (2)$$

where  $M_8$  is the mass of the central blackhole in the unit of  $10^8 M_\odot$ .  $R_{pc}$  and  $D_{pc}$  are in the unit of pc.

On the other hand, if the iron line comes from the same absorbing matter, the ionization parameter  $\xi \equiv L/nR^2$  of the matter should be  $\xi < 100 \text{ erg cm s}^{-1}$ , since the energy of the detected iron K line was 6.4 keV (see section 5.4) suggesting that the matter was cold or slightly ionized (Kallman & McCray 1982). Here  $n$  is the density of the plasma. Assuming the number of the clouds in the line-of-sight to be  $N_c$ , the observed column density  $N_H$  was the sum the densities of the clouds,  $N_H = N_c n D$ . Substituting the source X-ray luminosity of  $L = 3 \times 10^{43} \text{ erg s}^{-1}$  and  $N_H = 1 \times 10^{23} \text{ cm}^{-2}$ ,

$$D_{pc} < 1.0 R_{pc}^2 N_c^{-1}. \quad (3)$$

Eq. (1) and (3) give the upper limit of  $D_{pc}$  as

$$D_{pc} < 5 \times 10^{-3} M_8^{2/5} N_c^{-1/5}.$$

The maximum value is at  $R_{pc} = 0.07 M_8^{1/5} N_c^{2/5}$ .

Eq. (2) and (3) give the lower limit of  $R_{pc}$  as

$$R_{pc} > 0.011 M_8^{1/5} N_c^{2/5}.$$

Since the dependencies of  $M_8$  and  $N_c$  are weak,  $R_{pc}$  is consistent with the putative obscuring torus.

Eq. (1) and (3) also give  $D/R < 0.07 M_8^{1/5} N_c^{-3/5}$ , which is consistent with the view that there are many ( $\sim 10$ ) small (compared with the size of the torus) clouds near the edge of the torus. The transverse motion of the clouds could cause the observed change of the column density. The number of the clouds in our line-of-sight

Fig. 5. Confidence contour levels (68%, 90% and 99%) for the spectral slope vs. the intrinsic absorption column density. The solid and dashed lines are for AO4 and AO2 data, respectively. The photon-indices of the hard continuum are in the range of 1.3-1.6 in the two datasets. The intrinsic absorption changed evidently 44% in the 2 year interval.

Fig. 6. Comparison of the rapid-variability characteristics of NGC 7582 seen in 2–10 keV with Seyfert 1 galaxies (Nandra et al. 1997), on the basis of 128 s temporal analysis. Also shown in the figure, three other type-2 objects: NGC 526A, MCG-5-23-16 and NGC 7314 (Turner et al. 1997a). For these Seyfert 2 galaxies, the rapid variability alone suggests that the hidden Seyfert 1 nuclei are directly seen in the hard X-rays.

is large enough that NGC 7582 almost always shows the similar absorption feature.

In the present case, the significant column variations were observed on a timescale of years, therefore supporting the association of the X-ray absorbing matter with the putative torus. However, more tight constraints on the physical conditions of the absorbing material can be expected from the future observations with time scales of week  $\sim$  year.

### 5.3. The spectral components

#### 5.3.1. The origin of soft emission

The lack of rapid variability in the soft X-ray band suggests that it has a different origin from the hard continuum. Some origins, either electron scattering, thermal emission, or a mixture of the two, are expected to explain it.

There are good evidence for starburst activities undergoing in the center region of NGC 7582. For examples, the optical spectrum of NGC 7582 shows high-order Balmer absorption features, which Ward et al. (1980) interpreted as evidence for a significant population of hot stars; also its infrared spectrum is dominated by dust emission, and shows both dust emission and silicate absorption features (Roche et al. 1984). However, we found that the thermal emission related to this starburst activities can not explain the total soft X-ray excess. According to the far-infrared(FIR)/X-ray luminosity correlation for normal and starburst galaxies (David, Jones & Forman, 1992), we estimated, from the FIR luminosity of NGC 7582, the maximum expected starburst contribution to the 0.5–4.5 keV luminosity is  $\sim 1.7 \times 10^{40}$  erg s $^{-1}$ , which is 3–5 factors below the derived luminosity of the

soft X-ray component in the thermal (e.g. Raymond-Smith) model (see section 4.1). Furthermore, the acceptable fits obtained with a RS thermal model need an abnormally low metal abundances, less than 0.08 solar values (see table 1), this is unlikely to be real, because all known abundance gradients in spiral galaxies suggest that the nuclei should be somehow enriched in heavy elements with respect to solar (e.g. Vila-costas & Edmunds, 1992). There is one possibility to explain this low metal abundance, i.e. the soft emission is a mixture of thermal component with a featureless continuum, e.g. the scattered nuclear emission. However, in this case, the thermal component with normal metal abundance no more dominates the soft emission. All these results make the hypothesis of a major thermal origin for the soft excess to be unlikely in NGC 7582.

As shown in section 4.2, the soft excess emission of NGC 7582 showed complex and composite spectrum, either the unique thermal or scattered origin can be rejected by the data. We concluded that the soft spectrum is dominated by the scattered component with 10–20% contribution from the starburst emission. The “scattering efficiency”, as defined by the normalization ratio of the scattered to the primary power-law continuum, was found to be of 3-4%. Similar properties of the spectrum at low energies were also found for many others Seyfert 2 galaxies (Ueno 1997; Turner et al. 1997a), with the statistical distribution of scattering efficiencies in the range of 1–10%.

The scattered view of the major soft X-ray emission of NGC 7582 was also expected by the presence of non-thermal UV emission (Kinney et al. 1991; Mulchaey et al. 1992), which could not be seen through an absorption of

$\sim 10^{23} \text{ cm}^{-2}$ . Thus it should be a scattered light of nuclear emission. One can expect that several soft emission lines will be produced in the warm gas which is responsible for the scattering, as seen in the ASCA spectra of Mrk 3 (Iwasawa et al. 1994; Turner et al. 1997b). It is, however, hard to discriminate such photoionized lines in the present data, because of the poor statistics and contamination by the thermal starburst emission.

The present data showed evidently a scattered and obscured view of a hidden Seyfert 1 nucleus. This naturally suggested that a hidden broad line region (HBLR) should also be detected in the polarized spectrum in the context of the unified model for Seyfert galaxies. However, Heisler et al. (1997) reported recently a non-detection of polarized broad emission lines (PBLs) for NGC 7582 in a well defined infrared-selected sample of Seyfert 2 galaxies. On the one hand, there are difficulties in measuring weak PBLs, and we have little knowledge on how well the visibility of HBLR in Seyfert 2 galaxies is related to their X-ray properties.

### 5.3.2. The flat continuum

The best-fit model for both observations require a strongly absorbed hard power-law continuum. Figure 5 shows that, within the 99% error range, the two observations are consistent with a photon index of  $\Gamma \sim 1.3 - 1.6$ . This indicates that the primary X-ray spectrum of NGC 7582 is rather hard compared with the averaged slope ( $\Gamma \approx 2.0$ ) found for most of other Seyfert 2s (Turner et al. 1997a). It is well established that presence of reflecting matter in the nuclear region could strongly flatten the observed AGN continuum (Lightman & White 1988; George & Fabian 1991; Matt Perola & Piro, 1991), and Ginga observations of some Seyfert galaxies supported this idea (Matsuoka et al. 1990; Pounds et al. 1990).

We have tried to add a reflection component (“ploreff” model in XSPEC) in the best-fit model to test the possibility that the apparent flat spectrum could be due to an intrinsic steep continuum plus some cold reflection. The result (e.g. for AO4 data) showed that an intrinsic steep continuum with  $\Gamma \approx 1.85 \pm 0.28$  plus a certain reflection ( $R \approx 0.88 - 4.22$ ) slightly improved the spectral fit at  $\gtrsim 68\%$  confidence ( $\Delta\chi^2 = 2$  with one additional free parameter). Though the reflection ratio  $R$ , which describes the relative strength of reflection component to the direct component, was not tightly constrained, the present reflection model predicts an equivalent width of  $250 \pm 150$  eV for the iron line. This value is slightly larger than, but still consistent with the observed value of  $EW \approx 135_{-90}^{+30}$ .

An alternative possibility to flatten a steep intrinsic continuum is through the presence of an additional more strongly absorbed power-law. This scenario usually be referred as “Dual-Absorber” model, which can be related to a physical scenario for type 1.5/2 AGNs in which

the continuum source is completely covered by a torus of nonuniform density (see Weaver et al. 1994; Hayashi et al. 1996). We found that a dual-absorber model with an additional column of  $N_{\text{H}} \simeq 6.3_{-2.8}^{+3.5} \times 10^{23} \text{ cm}^{-2}$  could explain the data with a steep power-law component similar to the case of reflection model. The only constraint on such a complex model comes from the iron K absorption edge at  $\sim 7.1$  keV expected by neutral absorption. The model predicts an absorption edge with optical depth  $\tau \simeq 0.16 - 0.33$  (90 % confidence), which is still consistent with the measured value of  $\tau = 0.15_{-0.10}^{+0.15}$  (see section 4.2). Therefore, it seems that composite dual-absorber model is another plausible explanation for the flat continuum of NGC 7582. The same model has also been applied for several other sources observed with ASCA, like NGC 5252 (Cappi et al. 1996), NGC 2110 (Hayashi et al. 1996) and IRAS 04575-7537 (Vignali et al. 1998).

The remaining possible interpretation is that the spectrum is intrinsically flat. This will pose a serious problem for theoretical models which are successful in the explanation of AGN’s canonical X-ray slope at the value of  $\Gamma \simeq 1.9 - 2.0$  (e.g. see Haardt & Maraschi 1991; 1993). There seems increasing number of Seyfert 2 galaxies with flat spectra revealed by Ginga and ASCA, where Ginga data suggests that many of them can not be explained by the reflection model (Smith & Done 1996); however, ASCA data suggests that many of them tend to be explained by the dual-absorber model. Actually, so far no any case could clearly claim to exclude both possibilities due to the limit of data quality. Therefore, whether or not there are Seyfert galaxies with intrinsic flat spectra is still an open question.

### 5.4. The iron $K\alpha$ line feature

An iron  $K\alpha$  line emission was significantly detected in both observations. The best-fit line energy for both observations are consistent with the iron fluorescence line of 6.4 keV at rest from nearly-cold matter ( $< \text{Fe XVI}$ ) (e.g. Makishima 1986). The observed equivalent width of  $EW_{K\alpha} \simeq 100 - 200$  eV is slightly larger than the prediction ( $\sim 70-90$  eV) of the model where gas with inferred column density uniformly distributed around an isotropic X-ray source (e.g. Inoue 1990). It, however, can be easily interpreted by the model that the surrounding matter is not uniformly distributed, but in “torus” like geometry (Inoue et al. 1990; Awaki et al. 1991). In such a case, since the observed absorption is Compton-thin, and it is well believed that absorption tori in prototype Seyfert 2 galaxies are Compton-thick (i.e.  $N_{\text{H}} \gtrsim 10^{24} \text{ cm}^{-2}$ ), we probably observe the central source through the edge of the torus. The observed complex configuration of X-ray absorbing material along our line-of-sight, as suggested by its column variation as well as the sign of “dual-absorber”, can be understood by such a scenario.



We note that observed equivalent width of iron  $K\alpha$  is very similar to the average result of  $\langle EW_{K\alpha} \rangle = 160 \pm 30$  eV found for Seyfert 1 galaxies (Nandra & Pounds 1994; Nandra et al. 1997). There are strong evidence that iron  $K\alpha$  lines in Seyfert 1 galaxies are originated from an accretion disk near a supermassive black hole (Tanaka et al. 1995; Fabian et al. 1996). For Type 2 AGNs, both the accretion disk in the inner region and the torus in the outer region are expected to be the source of the line emission. In fact, that line complex emitted from the two distinct X-ray reprocessors within a single type 2 AGN was observed by ASCA (Weaver et al. 1997).

In the present case, the line width of  $\sigma_{K\alpha} = 0.15_{-0.07}^{+0.10}$  keV (FWHM  $\sim 9,000$ – $28,000$  km s $^{-1}$ ) is significantly broader than the instrumental response ( $\sigma \sim 50$  eV at 6 keV), but still much smaller than the mean width of  $\langle \sigma_{K\alpha} \rangle = 0.43 \pm 0.12$  keV found for the Seyfert 1 galaxies (Nandra et al. 1997b). Therefore, it is unlikely that disk-line component is important in NGC 7582. It could be the case that NGC 7582 has an edge-on accretion disk as generally expected for type 2 AGNs, and that the ultra-broad weak line profile is smeared out with the continuum.

Line profile and variability studies provide determinative information on the origin of iron  $K\alpha$  line. Unfortunately, such examinations for the present datasets are inconclusive due to the limited energy resolution of the line measurements. Much progress are expected to be made from the future X-ray missions, such as AXAF, Astro-E and XMM.

## 6. CONCLUSION

Two ASCA observations on the Seyfert 2 galaxy NGC 7582 in 1994 and 1996 yield the following compelling results:

The hard X-ray (2–10 keV) flux was found highly variable on time scales as short as 5.5 hours for both observations; meanwhile the soft band (0.5–2 keV) flux remained constant in both observations. The different variabilities in the soft and hard fluxes indicate their different physical origins. Specifically, the rapid variability amplitude of the hard X-ray flux scaled by the source intrinsic luminosity are very similar to those of Seyfert 1 galaxies, implying it is the direct spectral component from the hidden Seyfert 1-like nucleus.

Time-averaged spectral studies revealed that the spectra, in the hard X-ray (2–10 keV) band, are best described by a flat ( $\Gamma \sim 1.3 - 1.6$ ) power-law continuum (i.e. the direct/primary continuum) absorbed by a column density of  $0.8 \sim 1.3 \times 10^{23}$  cm $^{-2}$ . Though the slope is somewhat flatter than the average of other Seyfert 2 galaxies, the spectrum is consistent with a steep slope modified by a reflection or complicated absorptions (e.g. “dual-absorbers”) in the line-of-sight.

A line feature was fitted with the center energy of  $\sim 6.4$  keV and the equivalent width of  $\sim 170$  eV, which corresponds to the iron  $K\alpha$  emission from nearly-cold matter. This can be interpreted as the fluorescence emission from a non-uniformly distributed absorbing material in a “torus-like” geometry. However, the slightly broad line width (FWHM  $\sim 15,000$  km s $^{-1}$ ) could also be a sign of unresolved multi-origins for the observed iron K line. Future X-ray space missions with high energy resolution at this band could hopefully determine the line emission regions.

The soft X-ray (0.5–2 keV) emission in excess of the absorbed direct power-law continuum demonstrates a composite spectrum. The dominant component is most likely due to scattered emission from the nuclear continuum; the remaining contribution ( $\sim 20\%$ ) at this band comes from a starburst component with temperature of  $kT \approx 0.8$  keV. The lack of any rapid variability in this band supports this interpretation. Such a scattered view of the soft X-ray emission is also predicted for the Seyfert 2 galaxies in the unified AGN model.

A significant variation ( $\sim 4 \times 10^{22}$  cm $^{-2}$ ) in the absorption column was detected between the two observations in the 2-year interval. The variation timescale of  $\sim$ years might indicate that the X-ray absorbing material might be a “patchy-torus” composed of many individual clouds.

The measured column density implies the “torus” is Compton-thin. This might indicate that either this object lies at an intermediate inclination angle between Seyfert 1’s and a prototype Seyfert 2’s, or the obscuring torus is not always Compton thick. In any case, NGC 7582 is one of the typical examples of the Seyfert 2 galaxies which exhibit both obscured and scattered emission components in X-rays as predicted by the unification scheme for Seyfert galaxies. In many details, the ASCA observations of this source provided very good tests for the unified models.

We thank all the members of the ASCA team who operate the satellite and maintain the software and database. This research has made use of the NASA/IPAC Extra-galactic Database (NED) which is operated by the Jet Propulsion Laboratory, California Institute of Technology, under contract with the National Aeronautics and Space Administration. S.J.X. acknowledges the financial support from an exchange program between the Chinese Academy of Sciences (CAS) and RIKEN, and a partial support from the President Foundation of CAS. S.J.X. is currently belongs to BAC which is jointly sponsored by the Chinese Academy of Sciences and Peking University.

## References

- Antonucci R.R.J. 1993, ARA&A 31, 473
- Antonucci R.R.J., Miller J.S. 1985, ApJ 297, 621
- Arnaud K.A. et al., 1991, XSPEC User's Guide(ESA TM-09)
- Awaki H., Koyama K., Inoue H., Halpern J.P. 1991, PASJ 43, 195
- Burke B.E., Mountain R.W., Harrison D.C., Bautz M.W., Doty J.P., Ricker G.R., Daniels P.J. 1991, IEEE Trans. ED-38, 1069
- Cappi M., Mihara M., Matsuoka M., Brinkmann W., Prieto M.A., Palumbo G.G.C. 1996, ApJ 456, 141
- Charles P.A., Philips M.M. 1982, MNRAS 200, 263
- Crawford C.S., Fabian A.C. 1994, MNRAS 266, 669
- David L.P., Jones C., Forman W. 1992, ApJ 388, 82
- Fabian A.C., Nandra K., Reynolds C.S., Brandt W.N., Otani C., Tanaka Y., Inoue H., Iwasawa K. 1995, MNRAS 277, L11
- George I.M., Fabian A.C. 1991, MNRAS 249, 352
- Ghisellini G., Haardt F., Matt G. 1994, MNRAS 267, 743
- Hayashi I., Koyama K., Awaki H., Ueno S., Yamauchi S. 1996, PASJ 48, 219
- Heisler C.A., Lumsden S.L., Bailey J.A. 1997, Nature 385, 700
- Lawrence A., Papadakis I.E. 1993, ApJ 41, L93
- Leighly K.M., O'Brien P.T. 1997, ApJ 481, L15
- Lightman A.P., White, T.R. 1988, ApJ 335, 57
- Kallman T.R., McCray R.A. 1982, ApJs 50, 263
- Inoue H. 1990, in Proc. 23rd ESLAB Symp., ed. J. Hunt, B. Battrock, Paris: Eur. Space Agency. p783
- Iwasawa K., Yaqoob T., Awaki H., Ogasaka Y. 1994, PASJ 46, L167
- Maccacaro T., Perola G.C. 1981, ApJ 246, L11
- Makishima K. 1986, in The Physics of Accretion onto Compact Objects, ed. K. O. Mason, M.G. Watson & N.E. White (Berlin: Springer), 249
- Matsuoka M., Yamauchi M., Piro L., and Murakami T. 1990, ApJ 361, 440
- Matt G., Perola G.C., Piro L. 1991, A&A 247, 25
- Mulchaey J.S., Mushotszky R.F., Weaver K.A. 1992, ApJ 390, L69
- Mushotszky R.F. 1982, ApJ 256, 92
- Nandra K., Pounds K.A. 1994, MNRAS 268, 405
- Nandra K., George I.M., Mushotszky R.F., Turner T.J. & Yaqoob T. 1997a, ApJ 476, 70
- Nandra K., George I.M., Mushotszky R.F., Turner T.J. & Yaqoob T. 1997b, ApJ 477, 602
- Ohashi T., Ebisawa K., Fukazawa Y., Miyoshi K., Horii M., Ikebe Y., Ikeda Y., Inoue H., et al. 1996, PASJ 48, 157
- Osterbrock D.E. 1989, in *Astrophysics of Gaseous Nebulae and Active Galactic Nuclei*, (San Francisco: Freeman)
- Polletta M., Bassani L., Malaguti G., Palumbo G.G.C., Caroli E. 1996, ApJS 106, 399
- Pounds K.A., Nandra K., Stewart G.C., George I.M. 1990, Nature 344, 132
- Reichert G.A., Mushotszky R.F., Petre R., Holt S.S. 1985, ApJ 296, 69
- Roche P.F., Whitmore B., Aitken D.K., Phillips M.M. 1984, MNRAS 207, 35
- Serlemitsos, P., Ptak, A., Yaqoob, T. 1997, in The Physics of LINERs in View of Recent Observations, ed. M. Eracleous, A. Koratkar, C. Leitherer, & L. Ho, 70
- Stark, A.A., Gammie, C.F., Wilson, R.W., Bally, J., Linke, R.A., Heiles, C., Hurwitz, M. 1992, ApJS, 79, 77
- Storchi-Bergman T., Kinney A.L., Challis P. 1995, ApJs 98, 103
- Smith D.A., Done C. 1996, MNRAS 280, 355
- Tanaka Y., Inoue H., Holt S.S. 1994, PASJ 46, L37
- Tanaka Y., Nandra K., Fabian A.C., Inoue H., Otani C., Dotani T., Hayashida K., Iwasawa K., Kii T., Kunieda H., Makino F., Matsuoka M., 1995, Nature, 375, 695
- Turner T.J., Pounds K.A. 1989, MNRAS 240, 833
- Turner T.J. George I.M., Nandra K., Mushotszky R.F. 1997a, ApJS, 113, 23
- Turner T.J. George I.M., Nandra K., Mushotszky R.F. 1997b, ApJ, 488, 164
- Ueno S. 1997, Ph.D. Thesis, Kyoto University
- Vignali C., Comastri A., Stirpe G.M., Cappi M., Palumbo G.G.C., Matsuoka M., Malaguti G., Bassani L. 1998, A&A, in press
- Vila-Costas M.B. & Edmunds M.G. 1992, MNRAS 259, 121
- Ward M.J., Wilson A.S., Penston M.V., Elvis M., Maccacaro T., Tritton K.P. 1978, ApJ 223, 788
- Ward M., Penston M.V., Blades, J.C., and Turtle, A.J., 1980, MNRAS, 193, 563
- Warwick R.S., Pounds K.A., Turner T.J. 1988, MNRAS 231, 1145
- Warwick R.S., Sembay S., Yaqoob T., Makishima K., Ohashi T., Tashiro M., Kohmura Y. 1993, MNRAS, 265, 412
- Weaver K.A., Yaqoob T., Holt S., Mushotszky R.F., Matsuoka M., Yamauchi M. 1994, ApJ 436, L27
- Weaver K.A., Yaqoob T., Mushotszky R.F., Nousek J., Hayashi I., Koyama K. 1997, ApJ 474, 675

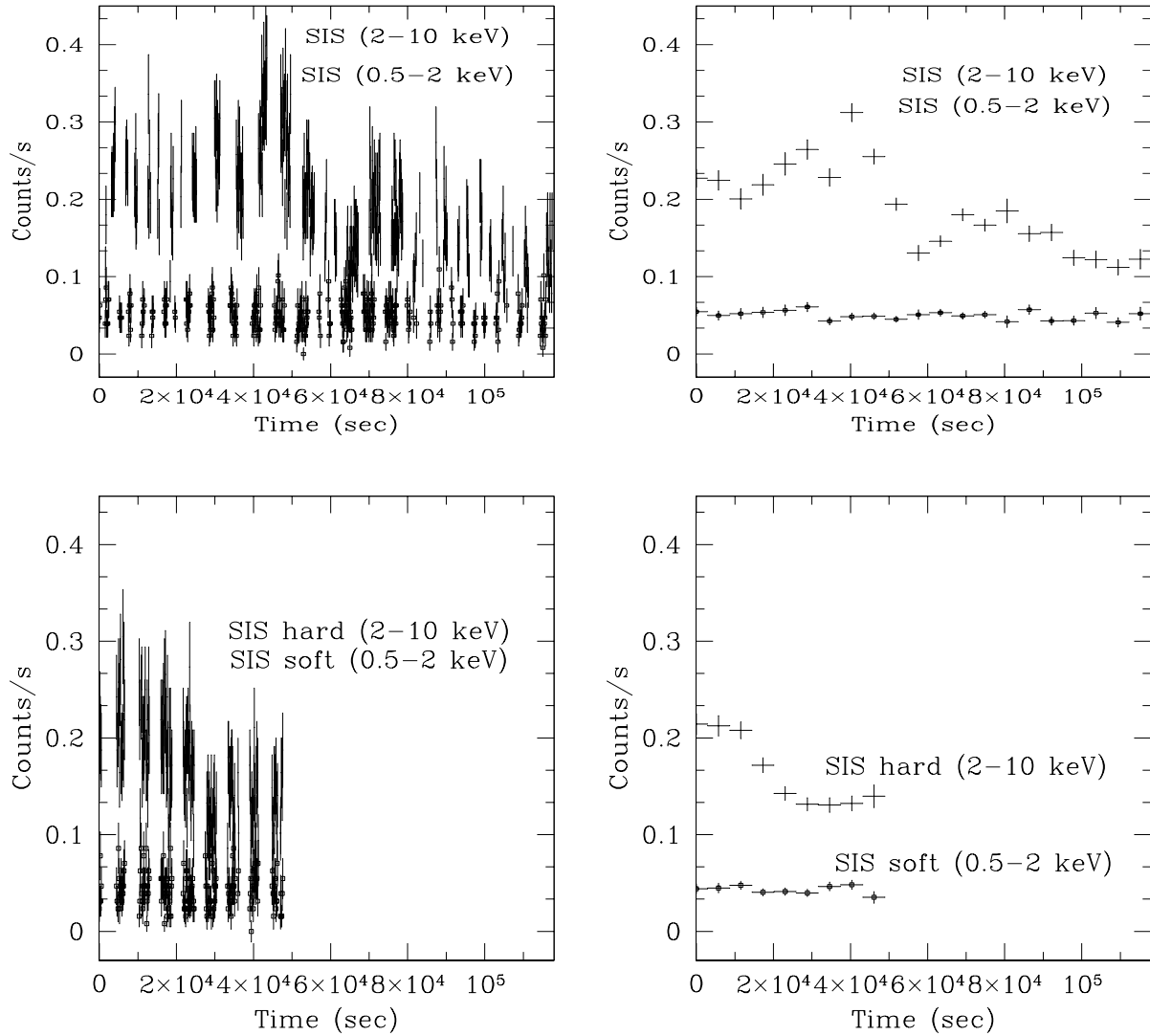


Fig. 1.— The comparison of SIS hard and soft band light curves of NGC 7582. Light curves in both short (128 s) and long (5760 s) bins are shown for AO4 (upper panel) and AO2 (lower panel), respectively. The time axis of AO4 starts from 18:24:13, November 21 (UT), 1996; and AO2 starts from 05:47:32, November 14 (UT), 1994. For both observations, the rapid variability is seen in the hard (2–10 keV) band, and no significant correlated variability in the soft (0.5–2 keV) band.

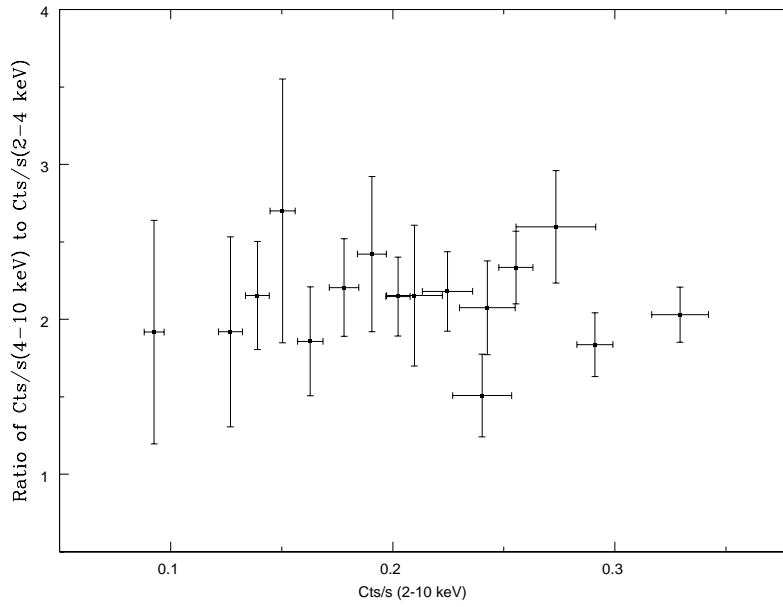


Fig. 2.— The hardness ratio (4–10 keV)/(2–4 keV) as the function of SIS count rate (2–10 keV) in AO4. No spectral variability, such as a change of  $N_{\text{H}}$ , was detected in the hard component.

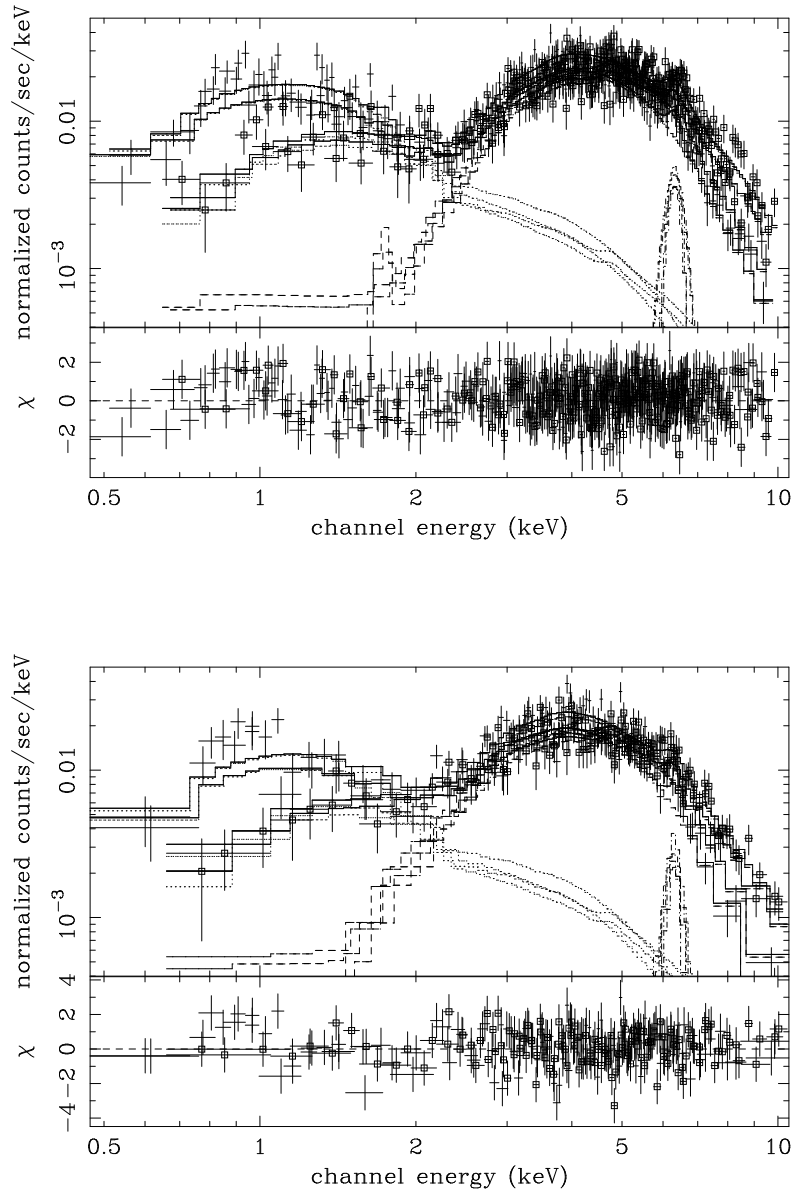


Fig. 3.— The folded spectrum of NGC 7582, fitted simultaneously for SIS(0/1) and GIS(2/3), with the scattering model. Related residuals for AO4 (upper panel) and AO2 (lower panel) are also shown. The cross marker represents the SIS data, and the void-square denotes the GIS data. The model gives acceptable description of the data (see table 1), but still some residuals remain around  $\sim 1$  keV, indicating that the soft spectrum is more complex than just scattered component.

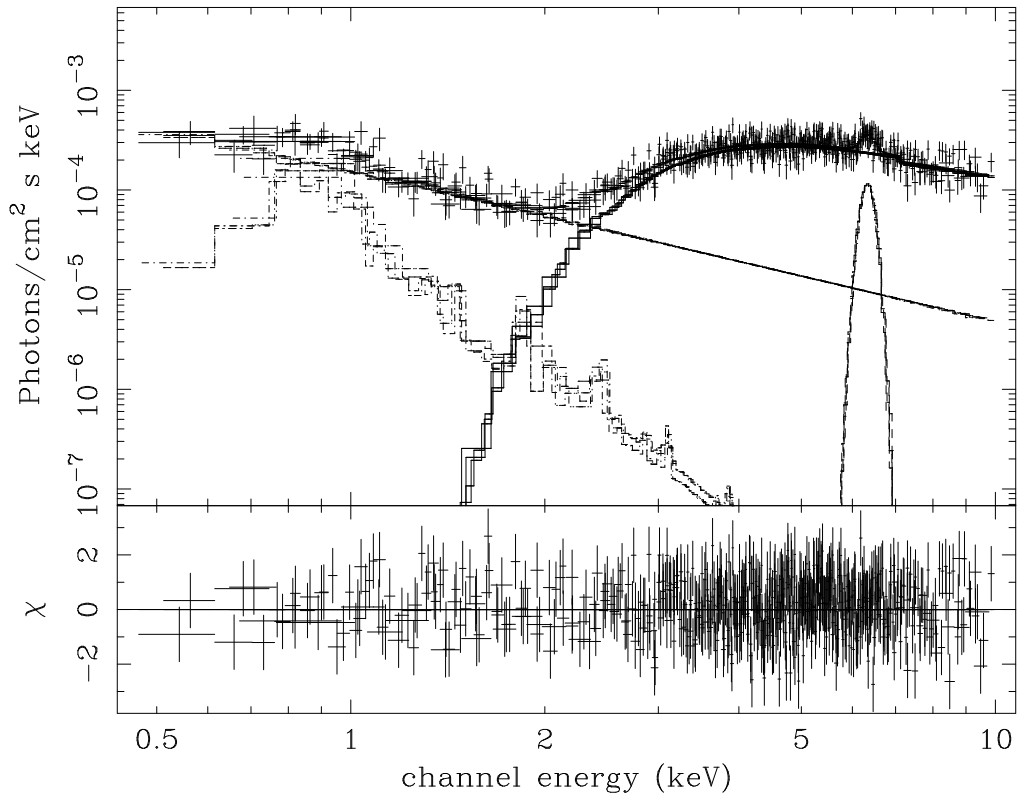


Fig. 4.— The unfolded spectrum shown for AO4, fitted with the model of “absorbed power-law + scattered power-law + Raymond-Smith + Fe K line”. The best-fit parameters of this model and flux measurements are listed in table 1 and table 2.

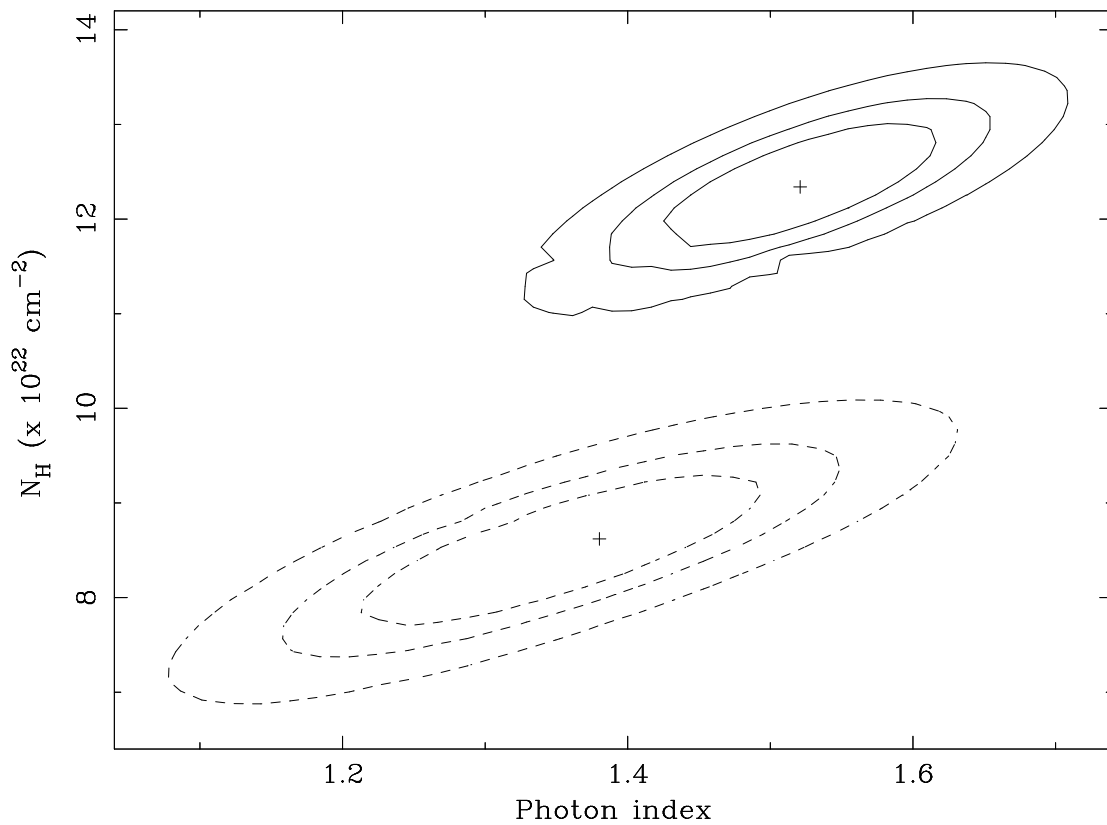


Fig. 5.— Confidence contour levels (68%, 90% and 99%) for the spectral slope vs. the intrinsic absorption column density. The solid and dashed lines are for AO4 and AO2 data, respectively. The photon-indices of the hard continuum are in the range of 1.3-1.6 in the two datasets. The intrinsic absorption changed evidently 44% in the 2 year interval.

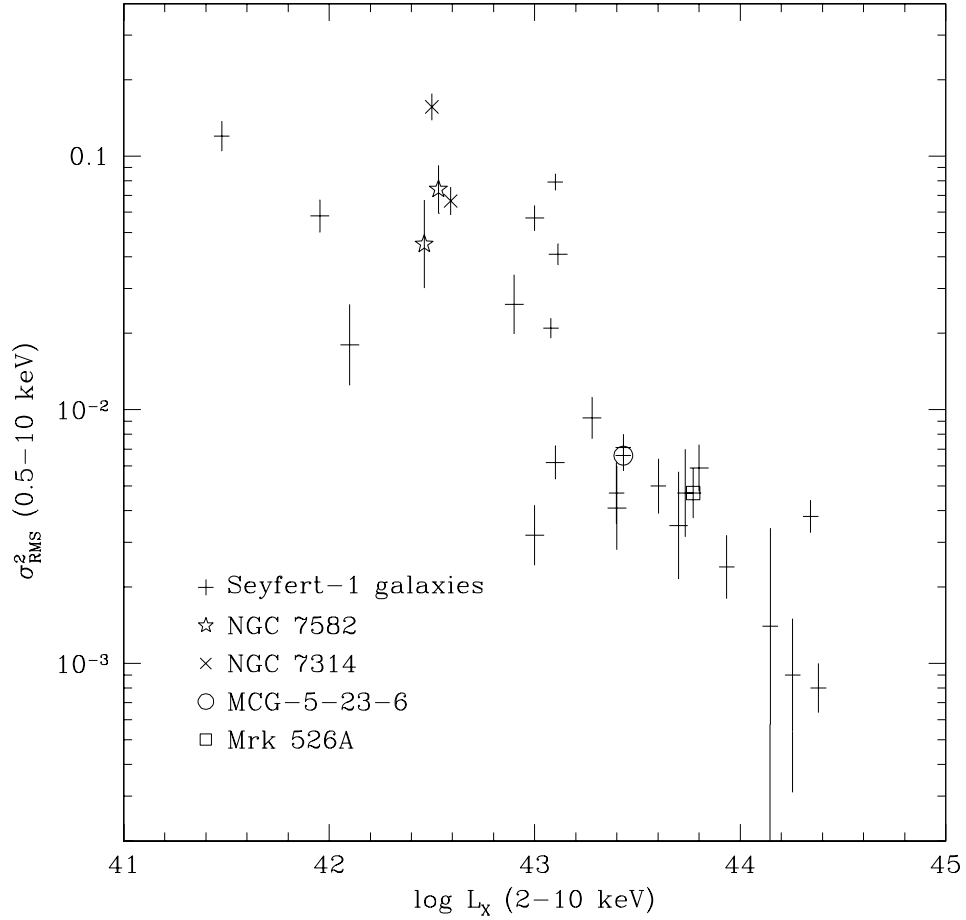


Fig. 6.— Comparison of the rapid-variability characteristics of NGC 7582 seen in 2–10 keV with Seyfert 1 galaxies (Nandra et al. 1997), on the basis of 128 s temporal analysis. Also shown in the figure, three other type-2 objects: NGC 526A, MCG-5-23-16 and NGC 7314 (Turner et al. 1997a). For these Seyfert 2 galaxies, the rapid variability alone suggests that the hidden Seyfert 1 nuclei are directly seen in the hard X-rays.